

**DESIGN AND KINEMATIC ANALYSIS OF A NOVEL SPHERICAL  
PARALLEL MANIPULATOR FOR LOWER LIMB EXOSKELETON  
APPLICATION**

Vamshi Krishna Lingampally<sup>1</sup>, Prof.Satish Babu Garlanka<sup>2</sup>

<sup>1,2</sup> *Mechanical Engineering Department, Jawaharlal Nehru Technological University*

**Abstract**—This project deals with the study of feasibility and later on design compact of a three DOF robotic joints to replace the single DOF of the hip actuator of the commercially available exoskeletons. In this project a novel spherical parallel manipulator (SPM), named Reflex with three degree-of-freedom (DOF) hip exoskeleton system that is capable of providing decoupled or combined 3-DOF rotational motion to a separate and passive target joint (i.e. the hip joint) is proposed. The kinematic analysis , performance Indices of the parallel manipulator are studied.

**Keywords** — spherical parallel manipulator (SPM ), Reflex, kinematic analysis, performance Indices.

**I. INTRODUCTION**

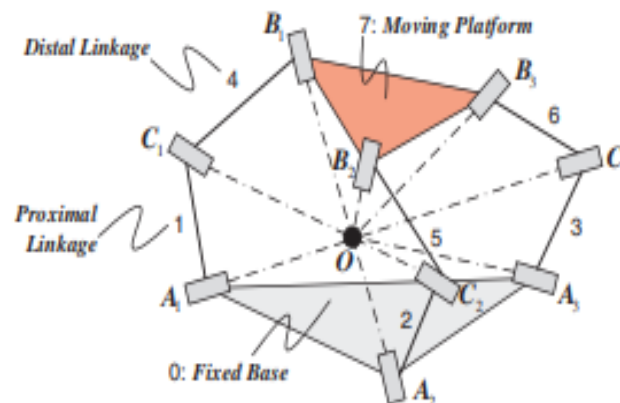
Numerous people require portability assistive advancements to stay aware of their day by day life and the interest for such gadgets ordinarily increments with age. A wearable exoskeleton robot is an outside basic mechanism with joints and links comparing to those of a human body. The exoskeleton specifically associates and synchronizes with human body to improve or bolster its normal developments so as to expand the absence of intensity in directing day by day exercises. The exoskeleton transmits torques from its actuators through unbending exoskeletal links to the human joints, in this manner giving versatility and enlarging the quality.

The most present-day exoskeletons are made out of kinematic open chains: sequentially associated single-DOF turning or kaleidoscopic joints between inflexible linkages. Be that as it may, parallel manipulators (PMs) have preferred execution over their sequential manipulator partners as to situating exactness, speed, constrain application, and payload-to-weight proportion. In this way, so as to enhance the automated execution and kinematic usefulness of exoskeletons, we propose the utilization of parallel robots combined with a mechanical structure that transmits movements to the focused on body part in an agreeable non-prohibitive way.

One parallel automated structure that has potential for use in such an application is the 3-RRR spherical parallel manipulator. This paper researches the execution of the 3-RRR with regards to exoskeleton applications. In particular, manipulability, expertise, and rotational affectability execution lists are assessed for two diverse body-interfacing plans of the manipulator when it is connected as a hip exoskeleton gadget; here it is accepted that the manipulator underpins 3-DOF rotational movements of the upper leg as for the pelvis. Our discoveries recommend that a 3-RRR manipulator can be utilized as the hip actuator in an exoskeleton framework.

**Kinematic considerations for the 3-RRR manipulator**

Kinematic architecture :

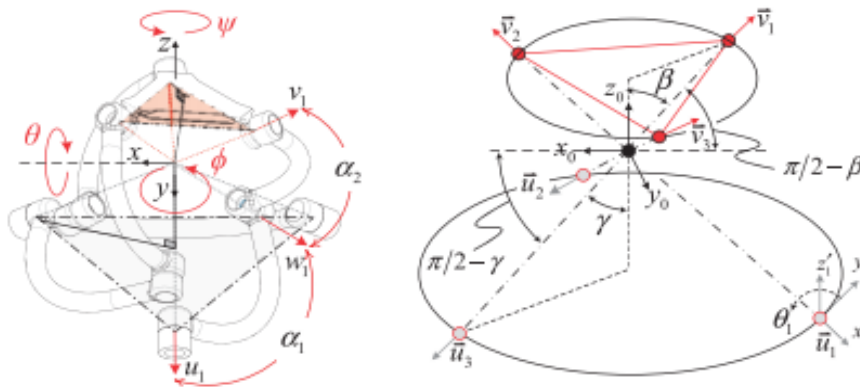


The above device is considered as a 3-DOF spherical system since the majority of its moving linkages perform spherical movements about a typical point, O, which is stationary as for its base structure. That is, every one of particles' movements inside the framework can be unambiguously portrayed by outspread projections on the surface of a unit circle focused at the previously mentioned stationary point. Subsequently, the main passable lower-pair joint inside a spherical

component's appendages is a revolute joint; besides, all joint tomahawks must converge at the regular stationary point referenced previously. Note that two striking encapsulations of the 3-RRR controller are the Agile Eye and Agile Wrist. Albeit mechanically particular, these two encapsulations have a similar converse kinematics strategy, which is surveyed further in the paper.

**INVERSE KINEMATICS DERIVATION**

The direction vectors  $u_1, u_2,$  and  $u_3$  specify the rotational axes of the system's three active  $A_i$  joints, as shown in Figure. These vectors have constant values with respect to the global frame (with origin O) because they correspond to fixed joints. Next, input scalar variables 1, 2, and 3 define the angular states of the respective active joints. Direction vectors  $w_1, w_2,$  and  $w_3$  in turn specify the rotational axes of the joints between the three proximal–distal link pairs (i.e. the  $C_i$  joints). These vectors vary in element values with respect to the global frame because they correspond to free joints. The final set of direction vectors,  $v_1, v_2,$  and  $v_3,$  specify the rotational axes of the joints between the three connection points of the distal links to the end effector (i.e. the  $B_i$  joints). Again, these vectors vary with respect to the global frame because they correspond to free joints.



Scalar constant  $\alpha_1$  specifies the angle between each actuated  $A_i$  joint and the corresponding proximal  $C_i$  joint within the plane containing both of these joints as well as the global origin O. The value of  $\alpha_1$  used for the 3-RRR design analyzed here is  $90^\circ$ . The second scalar constant  $\alpha_2$ , specifies the angle between each proximal  $C_i$  joint and the corresponding distal  $B_i$  joint within the plane containing both of these joints as well as the global origin. The value of  $\alpha_2$  used for the 3-RRR design considered here is also  $90^\circ$ . Third, scalar constant  $\beta$  indicates the angle between the  $v_i$  direction vectors and the global z-axis when the device is in its 'home' position (i.e. when the plane created by  $A_i$  joint positions is parallel to that defined by the  $B_i$  points). The value of  $\beta$  used here is  $54.75$ . Fourth, scalar constant  $\gamma$  indicates the angle between the  $u_i$  direction vectors and the vertical axis (i.e. the global z-axis). Unlike  $\beta$ , this value is constant for all mechanism states because the joints corresponding to the  $u_i$  direction vectors are fixed relative to the global frame. The value of  $\gamma$  used in this analysis is also  $54.75$ .

Finally, scalar constants  $\eta_1, \eta_2, \eta_3$  are used to specify the locations of the active joints associated with direction vectors  $u_1, u_2,$  and  $u_3$  and 'home positioned' distal passive joints associated with  $v_1, v_2,$  and  $v_3$  within the global x-y plane. Measured with respect to the positive y-axis, the values of  $\eta_1, \eta_2, \eta_3$  are  $0, 120,$  and  $240,$  respectively. Using this convention,  $\eta_i$  directly specifies the directions  $u_i$  in the global x-y plane and specifies the directions  $v_i$  in the global x-y plane when added to  $60^\circ$  and the mechanism is in its 'home' position. Note that the above parameter values are not independent, as they are related through geometry.

Equations for the  $u_i$  direction vectors can be derived in terms of the  $\eta_i$  and  $\gamma$  parameters discussed above. This derivation involves the following fixed-frame rotation process: rotation of a local frame  $F_1$  (i.e. originally identical to the global frame) by  $(90 - \eta)$  about the global  $^0y$ -axis and then rotation of  $F_1$  by  $\eta_i$  about the  $^0z$ -axis. This overall transformation is represented mathematically. Note that a superscript '0' indicates an axis or vector expressed with respect to the global frame.

$$R_{01} = R_z(\eta_i + 90^\circ)R_y(90^\circ - \gamma)$$

$$= \begin{bmatrix} -S\eta_i S\gamma & -C\eta_i & -S\eta_i C\gamma \\ C\eta_i S\gamma & -S\eta_i & C\eta_i C\gamma \\ -C\gamma & 0 & S\gamma \end{bmatrix}$$

It follows that the x-axis of the resulting  $R_{01}$  orientation frame is equal to the direction vector  $u_i$ .

$$u_i = \begin{bmatrix} -S\eta_i S\gamma \\ C\eta_i S\gamma \\ -C\gamma \end{bmatrix}^T$$

Direction vectors  $w_i$  are in turn related to the corresponding  $u_i$  vectors through a fixed rotation by  $\alpha_1$  within the plane containing O,  $A_i$ , and  $C_i$ , along with a variable rotation dependent on actuator angle  $\theta_i$ . The parameterization of this transformation can be considered as a set of current frame rotations: first a rotation of  $\theta_i$  about the local x-axis and then a rotation of  $\alpha_1$  about the updated local z-axis. In matrix format, an expression for this is as follows.

$$R_x(\theta_i)R_z(\alpha_1) = \begin{bmatrix} C\alpha_1 & -S\alpha_1 & 0 \\ -S\theta_i S\alpha_1 & -S\theta_i C\alpha_1 & -C\theta_i \\ C\theta_i S\alpha_1 & C\theta_i C\alpha_1 & -S\theta_i \end{bmatrix}$$

Now, to obtain expression in terms of the global coordinate system, the set of rotations described above must be pre-multiplied by  $R_{01}$ . Finally, the set of direction vectors  $w_i$  is obtained from the resulting matrix set as the x-axes for each  $W_i$ , as shown below.

$$w_i = \begin{bmatrix} (-S\eta_i C\gamma C\theta_i + C\eta_i S\theta_i)S\alpha_1 - S\eta_i S\gamma C\alpha_1 \\ (C\eta_i C\gamma C\theta_i + S\eta_i S\theta_i)S\alpha_1 + C\eta_i S\gamma C\alpha_1 \\ -C\gamma C\alpha_1 + S\gamma C\theta_i S\alpha_1 \end{bmatrix}^T$$

Similarly to the derivation for  $u_i$  vectors as summarized above, the  $v_i$  vectors can be established via two spatial rotations as follows when the device is in its 'home' position.

$$R_{03} = R_z(\eta_i)R_y(\beta)$$

Again,  $v_i$  is given as the x-axis component of the orientation matrix shown in equation . To determine the  $v_i$  directions after the mechanism's end-effector has undergone roll, pitch, and/or yaw rotations,  $R_{03}$  must be pre-multiplied by another transformation.

$$R_{04} = R_{rpy}R_{03}$$

where  $R_{rpy}$  represents the orientation of the end-effector with respect to the global frame. If it is assumed that  $R_{rpy}$  is expressed as fixed-frame rotations about the global x-axis by  $\theta$ , y-axis by  $\phi$ , and z-axis by  $\psi$ , respectively, then the  $v_i$  vector can be explicitly derived as follows.

$$\begin{bmatrix} v_{ix} \\ v_{iy} \\ v_{iz} \end{bmatrix} = \begin{bmatrix} 1 \\ 0 \\ 0 \end{bmatrix} \cdot R_z(\psi)R_y(\phi)R_x(\theta)R_{03}$$

Given that all direction vectors  $w_i$  and  $v_i$  are of unit length, the angle between corresponding  $w_i$  and  $v_i$  vectors is  $\alpha_2$  (by the parameter's definition), and the geometric definition of the vector dot product, the following equation relates the two sets of direction vectors.

$$w_i \cdot v_i = \cos\alpha_2 \quad i = 1, 2, 3$$

Now, through substitution of equations  $w_i$  and  $v_i$  into the above equation, a set of relationships between the system inputs and outputs is obtained. Upon performing this substitution and simplifying the result, the following equation is produced.

$$A \times \tan^2(\theta_i/2) + B \times \tan(\theta_i/2) + C = 0 \quad i = 1, 2, 3$$

Where

$$A = (-C\eta_i C\gamma S\alpha_1 + C\eta_i S\gamma C\alpha_1)v_{iy} + \dots (S\eta_i C\gamma S\alpha_1 - S\eta_i S\gamma C\alpha_1)v_{ix} + \dots (-C\gamma C\alpha_1 - S\alpha_1 S\gamma)v_{iz} - c\alpha_2$$

$$B = 2S\eta_i S\alpha_1 v_{iy} + 2C\eta_i S\alpha_1 v_{ix}$$

$$C = (-S\eta_i C\gamma S\alpha_1 - S\eta_i S\gamma C\alpha_1)v_{ix} + (-C\gamma C\alpha_1 + S\alpha_1 S\gamma)v_{iz} + (C\eta_i C\gamma S\alpha_1 + C\eta_i S\gamma C\alpha_1)v_{iy} - c\alpha_2$$

It follows that the input angle required to achieve a desired end-effector positional output can be found with the following equation.

$$\theta_i = 2 \operatorname{atan2} \left( \frac{-B \pm \sqrt{B^2 - 4AC}}{2A} \right) \quad i = 1, 2, 3$$

Above equations represent the solution to the inverse kinematics problem for the 3-RRR manipulator because they provide the required active joint states,  $\theta_i$ , necessary to achieve a desired orientation of the end-effector. That is, once end-effector rotations  $\theta, \phi$  and  $\psi$  are established, the associated angular states of the active revolute joints can be identified.

**Jacobian analysis**

A number of generally accepted performance indices for parallel manipulators are often published as a method for comparing various robotic manipulators. The values of these indices usually have physical significance and applications for design optimization. The three indices considered in this paper, which are manipulability, dexterity, and rotational sensitivity, all derive from the Jacobian matrix of a manipulator. Thus, the 3-RRR device's Jacobian development is discussed in this section, before the performance indices are examined in the next section. To start, a vector  $q$  is assigned to represent active joint variables while  $x$  is used to characterize the end-effector's position. The kinematic constraints associated with the device's limbs can be expressed as follows.

$$f(x, q) = 0$$

Where  $f$  is an  $n$ -dimensional implicit function of  $q$  and  $x$ , and  $n$  is the active joint count within the mechanism. Now, time-differentiating equation yields the following relationship between input joint rates and end-effector velocity.

$$\frac{\partial f}{\partial x} \dot{X} + \frac{\partial f}{\partial q} \dot{q} = 0 \rightarrow J_x \dot{X} = J_q \dot{q}$$

As shown above, two components of the Jacobian are produced:  $J_x$  and  $J_q$ . The combination of these components yields the complete Jacobian matrix.

$$\dot{q} = J_q^{-1} J_x \dot{X} = J \dot{X}$$

It is important to note that the Jacobian associated with a parallel manipulator, as in above equation is derived as the inverse of a serial manipulator's Jacobian.

when equation is written once for each of  $i=1, 2$ , and  $3$  three scalar equations are produced. These can be arranged in matrix form as follows.

$$\begin{bmatrix} (w_1 \times v_1)^T \\ (w_2 \times v_2)^T \\ (w_3 \times v_3)^T \end{bmatrix} \omega_b = - \begin{bmatrix} w_1 \times u_1 \cdot v_1 & 0 & 0 \\ 0 & w_2 \times u_2 \cdot v_2 & 0 \\ 0 & 0 & w_3 \times u_3 \cdot v_3 \end{bmatrix} \dot{q}$$

Combining both of the above equations yields a complete form of the 3-RRR manipulator's Jacobian matrix.

$$J = J_q^{-1} J_x = - \begin{bmatrix} w_1 \times u_1 \cdot v_1 & 0 & 0 \\ 0 & w_2 \times u_2 \cdot v_2 & 0 \\ 0 & 0 & w_3 \times u_3 \cdot v_3 \end{bmatrix}^{-1} \times \begin{bmatrix} (w_1 \times v_1)^T \\ (w_2 \times v_2)^T \\ (w_3 \times v_3)^T \end{bmatrix}$$

Recall that vectors  $u_i, w_i$ , and  $v_i$  which can be computed from above equations respectively.

**Hip exoskeleton design based on performance indices**

With the 3-RRR manipulator's Jacobian matrix derived, it is now possible to evaluate several of the device's performance indices. In doing so, two methods for attaching the device to the human body are considered, as shown in Figure . Furthermore, only flexion-extension and abduction-adduction motions are considered; the final major DOF of the hip joint (i.e. internal/external rotation) is assumed to be constant and oriented such that the knee's axis of rotation is perpendicular to the sagittal plane of the body. As can be deduced from Figure , the device's  $\psi$  angle corresponds to flexion/extension motions for Attachment Method 1, while  $\phi$  is associated with those motions in Attachment Method 2; for both cases,  $\theta$  corresponds to abduction/ adduction motions. Additionally, a workspace range of  $[-0.2 \ 0.2]$  radians for both flexion-extension and abduction-adduction motions was considered for all local performance studies. Finally, the results below are only applicable when the parameter values (i.e. for  $\alpha_1, \alpha_2, \beta, \eta_1, \eta_2, \eta_3$ ) are selected as per the discussion in Kinematic architecture section.

**Manipulability**

Forces experienced by joints within parallel manipulators tend to become large when such a device nears singular configurations. Thus, the ability to quantify a manipulator's nearness to singular configurations is useful. Manipulability is a common performance index used to accomplish this quantification. It is defined as the absolute value of the Jacobian's determinant, as given in equation . Alternatively, this index can be interpreted as the Jacobian matrix's minimum-magnitude eigen value.

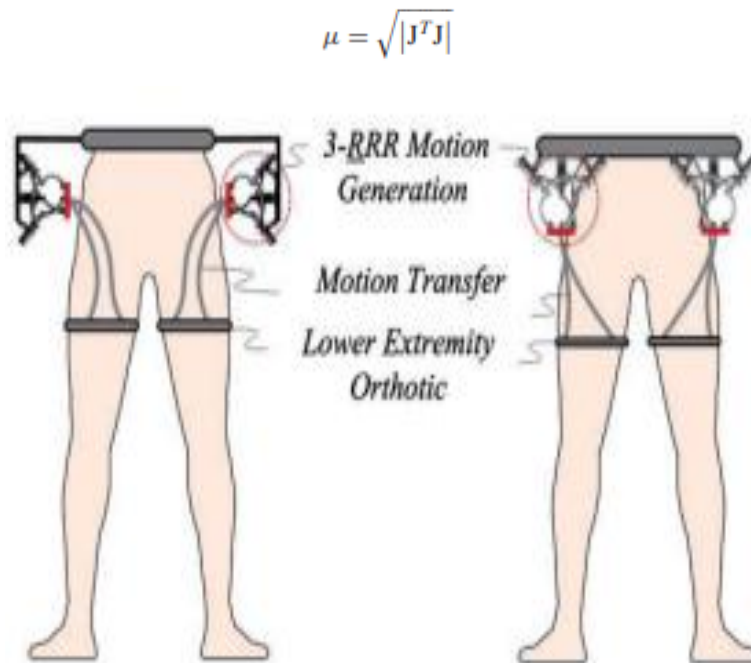


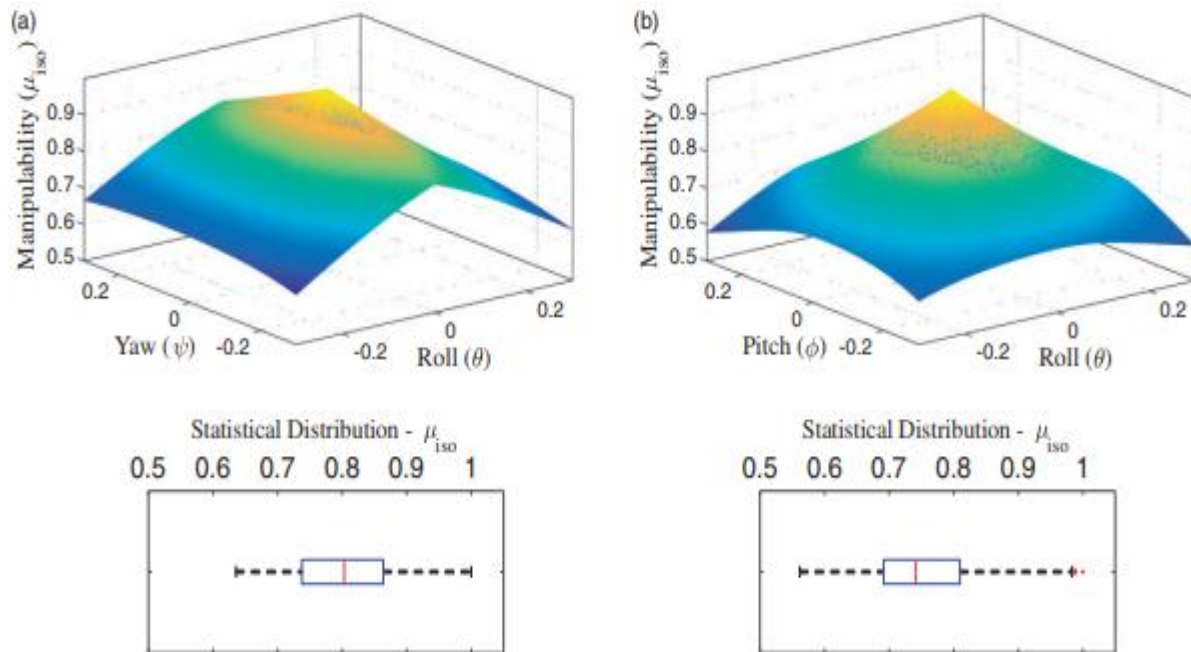
Fig.(1) Considered 3-RRR attachment methods as a hip exoskeleton. (a) Interfacing scheme 1; (b) interfacing scheme 2

In mechanical terms, manipulability represents a manipulator's ability to successfully create a desired velocity at its end-effector. Alternatively, this index can be understood as the ellipsoid volume resulting when a unit sphere is mapped from the manipulator's n-dimensional joint space into Cartesian space through its Jacobian matrix and a constant proportionality factor; recall that n represents the active joint count for the manipulator. It follows that a manipulator achieves greater manipulability performance if its ellipsoid has a greater uniformity, or isotropy, characteristic. Such an isotropy index for manipulability can be quantified as follows.

$$\mu_{iso} = \sigma_{min} / \sigma_{max}$$

where min and max are the minimum and maximum singular values of the Jacobian matrix, respectively. The  $\mu_{iso}$  value in above equation is limited to the range [0, 1], where 0 indicates inability to transmit velocity to the end-effector (i.e. a singular configuration) and 1 indicates ability to transmit velocity to the end-effector uniformly in all directions. The surface plot shows the 3-RRR device's manipulability deviation and statistical distribution within the considered workspace for the two attachment methods depicted in Figure 1. According to the surface plots below shown in fig 2, the manipulability of the 3-RRR is greatest when operating near its 'home' configuration and least near the boundaries of the considered workspace for both attachment methods. Comparatively, Attachment Method 1 achieves a greater average value for manipulability than Attachment Method 2. Furthermore, Method 1 achieves less variance in performance within the workspace considered. Therefore, Method 1 is superior to Method 2 in terms of manipulability.





. Fig(2) 3-RRR manipulability for (a) Attachment Method 1 and (b) Attachment Method 2.

**Dexterity (condition number)**

Because a manipulator’s control scheme generally relies on its joint position co-ordinates, any errors between the expected and actual joint coordinates cause errors in the end-effector’s position and orientation. This end-effector error can be determined through multiplication of the errors in the joint coordinates by a scaling factor: the condition number,  $k$ . A manipulator’s condition number is obtained from the Jacobian matrix as follows.

$$k(J) = \|J\| \|J^{-1}\|$$

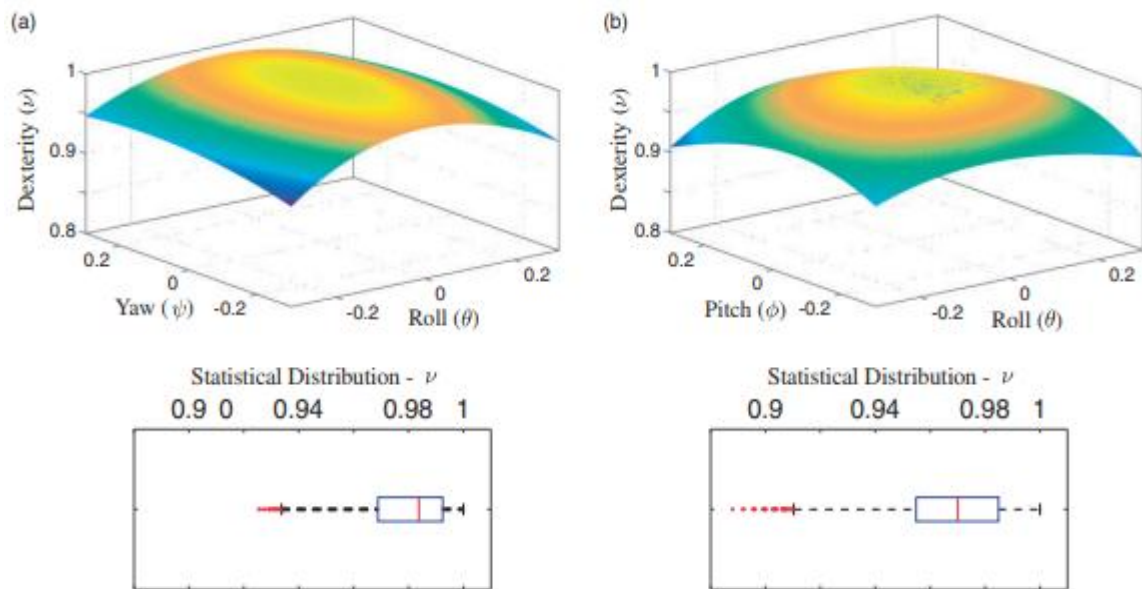
where  $J$  is the Jacobian matrix. Here,  $\|J\|$  denotes the Jacobian’s Euclidean norm.

$$\|J\| = \sqrt{\text{tr}\left(\frac{1}{n}JJ^T\right)}$$

Gosselin proposes that the condition number’s inverse be used to quantify a manipulator’s kinematic accuracy, this criterion is called the local dexterity index, denoted by .

$$v = \frac{1}{\|J\| \|J^{-1}\|}$$

Again, allowable values for  $n$  are constrained between 0 and 1; zero indicates a singularity, and greater values correspond to increasingly accurate motion generation at the end-effector. Surface plot in fig(3) depicts and statistical box plots depicts both body-attachment arrangements of the 3-RRR manipulator across its considered workspace. Similarly to manipulability, these plots suggest that the mechanism’s dexterity is greatest when configured in close proximity to its ‘home’ orientation and that it decreases as the device moves towards the boundaries of its considered workspace. Additionally, greater average dexterity and less dexterity variation are achieved when the 3-RRR robot is interfaced with the human body according to Attachment Method 1 as opposed to Method 2, which makes the former preferable.



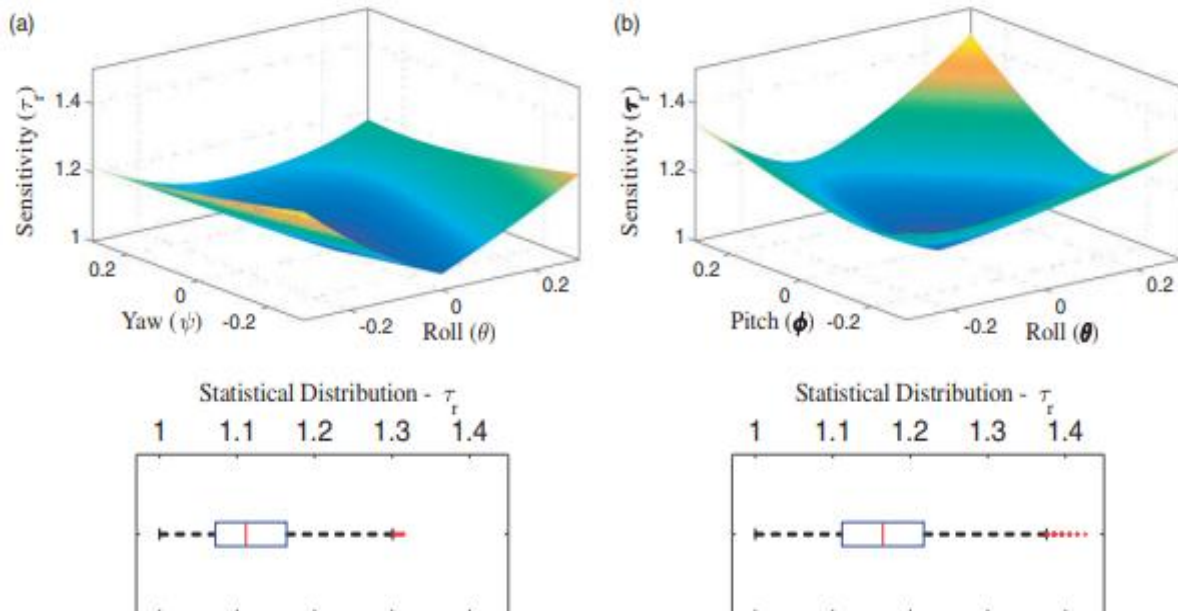
Fig(3) 3-RRR dexterity for (a) Attachment Method 1 and (b) Attachment Method 2

**Rotational sensitivity**

The rotational sensitivity index of a manipulator indicates how reactive its end-effector is to changes in active joint states. More specifically, it is the maximum-magnitude rotation of the end-effector under a unit-norm actuator displacement; it is given by either the 2–norm of the Jacobian matrix as follows.

$$\tau_r = \|J\|$$

Plots shows the sensitivity results for the 3-RRR manipulator when subject to the body-interfacing schemes of Figure 1 and constrained to the  $[-0.2 \ 0.2]$  radian workspace range in both flexion-extension and abduction-adduction motions. Again, Attachment Method 1 demonstrates preferable performance to that of Method 2 because the former possesses the smaller-magnitude average and variance range in sensitivity index value. Furthermore, sensitivity performance is optimal for both arrangements near the device’s ‘home’ orientation and degrades as the workspace limits are approached.



Fig(4) 3-RRR rotational sensitivity for (a) Attachment Method 1 and (b) Attachment Method 2.

**Conclusion and future work**

This paper proposes the use of the well-established 3-RRR manipulator as a robotic component within a hip exoskeleton system. Before investigating the mechanism’s performance for two different body-attachment methods the the device’s inverse kinematics and Jacobian matrix development procedures were revisited. The performance study results indicate that the body-interfacing arrangement that orients the manipulator’s x-y plane parallel to the body’s sagittal plane is superior in terms of average value and variability for manipulability, dexterity, and rotational sensitivity indices. As can be expected, the manipulator’s performance is optimal when configured at its initial ‘home’ orientation and degrades as the end-effector moves away from this state.